Green Chemistry

Accepted Manuscript

ROYAL SOCIETY OF CHEMISTRY

www.rsc.org/greenchem

Journal Name

RSCPublishing

ARTICLE

TPPS supported on core-shell PMMA nanoparticles: the development of continuous-flow membrane-mediated electrocoagulation as photocatalyst processing method in aqueous media†‡

Cite this: DOI: 10.1039/xoxxoooooox

Received ooth January 2012,
Accepted ooth January 2012

DOI: 10.1039/xoxxoooooox

www.rsc.org/

Paolo Dambruoso,*[a] Marco Ballestri,[a] Claudia Ferroni,[a] Andrea Guerrini,[a] Giovanna Sotgiu,[a] Greta Varchi,[a] and Alessandro Massi*[b]

The successful utilization of core shell poly-methyl methacrylate nanoparticles (CS-PMMA NPs) as valuable support for organocatalyst immobilization in water medium is herein presented along with an unprecedented direct current-based electrochemical method for processing the water colloid of the resulting nano-supported catalyst. The NP coagulation procedure relied on a variant of the electrocoagulation technique and it was effected through water electrolysis occurring in a dialysis membrane immersed in the colloid. NPs mass recoveries up to 95% w/w were obtained within 1 h electrolysis. This was optimized at 90 mA constant current or 24 V constant potential. The disclosed NP separation procedure was effectively exploited in a continuous-flow reaction/separation/recycle sequence involving the tetraphenylporphyrin tetrasulfonate (TPPS) organo-photocatalyst immobilized on CS-PMMA NPs (**NP2s**). After an optimization study aimed at maximizing the chemical efficiency of the whole synthetic and purification process, the nano-supported catalyst **NP2** (0.05 mol%) proved to efficiently promote the photoexcitation of triplet oxygen to singlet oxygen for the selective and environmentally benign sulfoxidation of a model sulfide in water medium.

Introduction

The development of innovative synthetic and purification procedures is continuously stimulated by increasing competition in which time, cost, and sustainability are crucial issues even at a research stage.[1] In this scenario, heterogeneous organocatalysis[2] is emerging as an attractive methodology offering unique opportunities for highly selective, metal-free syntheses facilitated by the ease of product/catalyst separation and catalyst recycling. Heterogeneous organocatalysis is typically conducted on micrometric supports, both under batch[3] and flow conditions,[4] while remaining less explored on the nanometric scale,[5] where the benefits of the 'semi-heterogeneous'[6] nature of the catalyst are amplified. Nanocatalysis[7] is a rapidly growing area of research, entailing the development of effective, low-cost techniques for nanoparticle (NP) processing. Magnetic separation has been shown to be a particularly efficient method,[8] other approaches include the immobilization of NPs on solid support, NP extraction from immiscible multiple phases, NP precipitation/redispersion, centrifugation, and filtration.[9] Fixed-bed reactors packed with mesoporous support-stabilized NPs[10] or dendrimer-encapsulated nanoclusters[11] have been used as well. The recently disclosed electropurification technique,[12] a reversible version of electrophoretic deposition (EPD),[13] also displays valuable attributes such as rapidity, efficiency, and use under batch or flow conditions.[14] Nevertheless, the requirement for high potentials appears as an important limitation of this technique for synthetic applications in aqueous media. Indeed, Joule heating of colloids,[13] release of metallic impurities from the electrodes, electro-osmotic flow, and gas evolution may result during EPD of aqueous colloids.[15] This may lead to problems in the recovery of water-dispersed nanocatalysts, highlighting the need for a NP purification/recycling electrochemical technique compatible with aqueous systems. This necessity became apparent to us at the beginning of a new research program aimed at demonstrating the potential of core-shell (CS) poly-methylmethacrylate (PMMA) NPs (Figure 1) as inert, inexpensive, and widely applicable nano-support for (organo)catalyst immobilization in water media. Our groups, in

fact, are currently active in the field of heterogeneous organocatalysis[16] and in the utilization of CS-PMMA NPs as carriers of anticancer drugs,[17] fluorophores, and photosensitizers[18, 19] for nanomedicine applications.

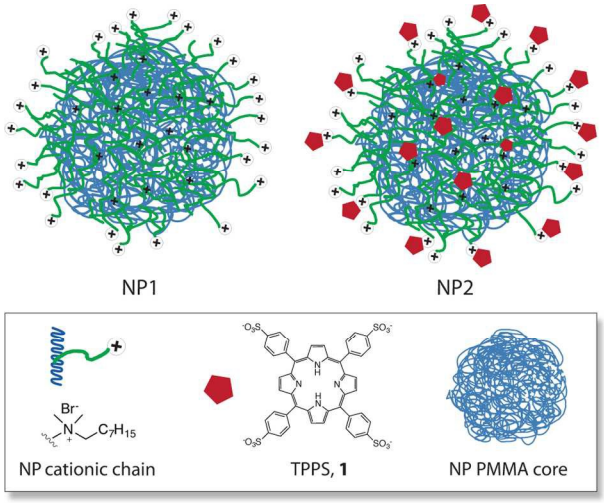

Figure 1. Core-shell poly-methylmethacrylate (CS-PMMA) nanoparticle (**NP1**), tetraphenylporphyrin tetrasulfonate anion (TPPS, **1**), and organo-photocatalyst (**NP2**).

The simple synthesis from readily available starting materials affording positively[17,20] or negatively[21] charged NPs with tunable dimensions as well as the water compatibility and ease of the immobilization procedure are attractive features of CS-PMMA NPs. In particular, nanoparticles **NP1s** displaying quaternary ammonium salts on their shell can be electrostatically conjugated[22] to sulfonated compounds such as the tetraphenylporphyrin tetrasulfonate anion (TPPS) **1** to give the nano-supported species **NP2** in a straightforward manner (Figure 1). Nevertheless, the difficult processing of **NP1** water colloids by standard procedures constitutes a major drawback for utilizations as catalyst support in synthetic applications. Centrifugation is precluded for **NP1** colloids with hydrodynamic diameter (d_h) below 100 nm;[23] at the same time, the use of membrane filters represents a costly solution, which also limits the scalability and practicality of the purification process. On the other hand, usage of flocculating agents may complicate the catalyst recycling step.

Within this framework, we describe herein a proof-of-concept study introducing the above-mentioned nano-supported porphyrin **NP2** as organo-photocatalyst for the highly selective in-water oxidation of a model sulfide with air under batch and flow regimes. Central in this research has been the development of a new procedure for nanocatalyst recovery/recycling based on electrocoagulation (EC).[24] While typical EC protocols use sacrificial anodes to induce NP sedimentation thus causing the release of metal hydroxide in the flocks, here this process has been effected through water electrolysis at electrodes suitably separated from the colloid bulk by an ion-permeable membrane. As widely discussed below, **NP2** separation and recycling could be achieved by this strategy in a mild, inexpensive, and environmentally benign fashion, using batch and continuous-flow experimental set-ups.

Results and discussion

Nanoparticles synthesis and characterization

Positively charged **NP1s** were prepared by emulsion polymerization of methyl methacrylate **5** in the presence of the cationic initiator 2,2'-azobis (isobutyramidine) dihydrochloride (AIBA), water, and the ionic comonomer 2-(dimethyloctyl) ammonium ethylmethacrylate bromide **4** (Scheme 1).

This emulsion stabilizer was obtained as previously described[17,20] by *N*-alkylation of 2-(dimethylamino)ethyl methacrylate **2** with 1-bromooctane **3** using 2,6-di-*tert*-butyl-4-methylphenol (BHT) as radical scavenger.

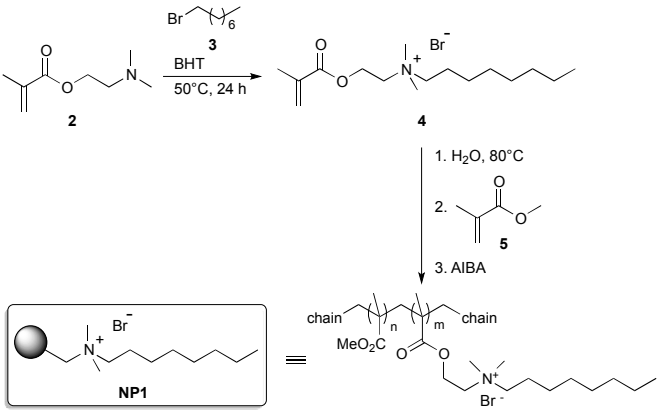

Scheme 1. Synthesis of nanoparticles **NP1s**.

Two batches of **NP1** colloids, namely **NP1s-(a)** and **NP1s-(b)**, were suitably synthesized by varying the composition of the polymerization mixture, and they differed in morphological and electrokinetic parameters, bromide loading, and concentration (Table 1).

Table 1. Features of nanoparticles **NP1s** and **NP2**s.

NPs samples	d_h [nm]	Z_p [mV]	Br^- [μmol/g]	*c* NPs [mg/mL]
NP1s-(a)	169 (0.11)[a]	57	381	30.3
NP1s-(b)	74.0 (0.10)[a]	32	688	14.6
NP2s[b]	109.9 (0.34)[a]	54	-[b]	2.9

[a]Polydispersity in bracket. [b]Colloid utilized in the optimized oxidation reaction depicted in Scheme 3 (TPPS **1** loading: 0.024 [μmol**1**/mg **NP1s-(b)**]).

The morphological characterization (SEM and AFM analyses) confirmed the spherical shape of both NPs (Figure 2), while the positive Zeta-potential (Z_p) indicated the presence of the quaternary ammonium salts on the external shell.[13] The molecular structure of **NP1-(a)** was confirmed by the combined analysis of the ^{1}H NMR, edHSQC, and HMBC spectra acquired on a freeze-dried sample dissolved in $CDCl_3$ (Figure 3). In details, signals at 0.85, 1.02, and 1.21 ppm of the ^{1}H NMR spectrum were assigned to the methyl protons of the

syndiotactic (rr), atactic (mr), and isotactic (mm) backbone units, respectively.[25] The bands in the range between 1.38-1.46 and 1.70-2.20 ppm were instead assigned to the methylene protons of the polymer backbone, as confirmed by the corresponding signals (52.0-56.0 ppm) in F1 of the edHSQC spectrum.

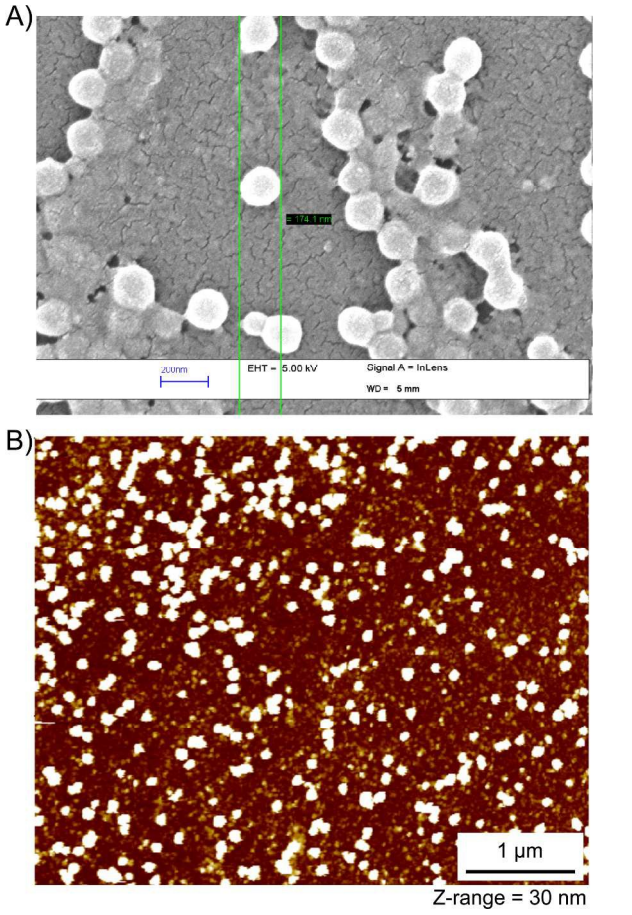

Figure 2. Morphological analysis of **NP1s**. A) SEM image of **NP1s-(a)**; B) AFM image of **NP1s-(b)**.

Furthermore, the methyl protons correlated with the methylene carbons (52.0-56.0 ppm in F1 of the HMBC), and both the methyl and methylene protons correlated with the backbone quaternary carbons and the ester carbons of the polymer (44.0-47.0 and 176.0-180 ppm, respectively, in F1 of the HMBC map). Characteristic signals of the octyl pendant chain of the comonomer **4** were also evidenced. The terminal methyl protons (0.90 ppm, ^{1}H NMR spectrum; 14.6 ppm, F1 of the edHSQC) correlated with the two methylenes at 23.1 and 32.1 ppm, respectively (HMBC). These latter two carbons, together with other three carbons, were directly linked to the corresponding five methylene protons in the 1.23-1.48 ppm range of the proton spectrum. The remaining two methylene protons centered at 1.84 and 3.71 ppm correlated with the carbons at 23.4 and 66.1 ppm, respectively (edHSQC). Finally, the signal at 3.51 (^{1}H) and 51.9 (^{13}C) ppm were assigned to the methyl groups of the quaternary ammonium salt.

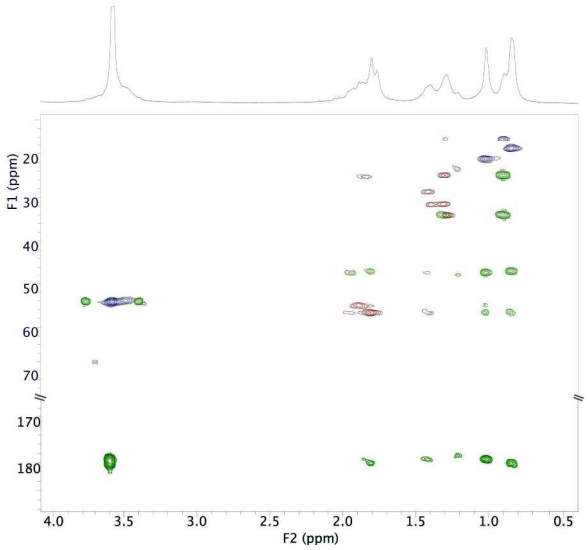

Figure 3. Overlapped ^{1}H NMR, edHSQC and HMBC of **NP1s-(a)**. edHSQC methyls: blue; edHSQC methylenes: red; HMBC cross-peaks: green. Spectra registered at 25°C in $CDCl_3$.

Nanoparticles recovery by membrane-mediated electrocoagulation

As anticipated, a fundamental prerequisite of our general synthetic program was to find a suitable method for the recovery of **NP1** alone or loaded with TTPS, namely **NP2**. Hence, we first attempted electrophoretic deposition by directly immersing the electrodes in a colloid of **NP1s-(a)**. As expected, a constant direct current (DC) of 1 mA produced both water electrolysis and cathodic EPD of NPs, which was in turn perturbed by gases produced at the electrodes (section 3 in the ESI for details). Surprisingly, a concomitant sedimentation of **NP1s** occurred, which also led to the partial clarification of the colloid.[26] This intriguing result, which clearly indicated the existence of an electrocoagulation phenomenon, prompted us to discover how to increase sedimentation by limiting EPD and, at the same time, avoid NP remixing due to gas bubbling.

Colloid stability is strongly influenced by electrolyte concentration, coagulation being the result of an increase in ionic strength[27] and/or pH variation.[28] Thus, we envisaged that a proper control of the presence in the colloid bulk of protons and hydroxyl ions generated by water electrolysis could favor the quantitative coagulation of **NP1s-(a)**. In addition, we hypothesized that physical separation of the electrodes from the colloid bulk could allow H_2 and O_2 to vent without disturbing NP sedimentation. Hence, the use of an ion-permeable membrane to separate the colloid from the water electrolysis appeared particularly suitable for both purposes.

The lab-scale set-up employed to investigate the feasibility of our hypothesis was an inexpensive apparatus consisting of a separating funnel (volume = 10 mL) equipped with a thermostatic jacket and overflow pipe, a DC power supply, and an electrolytic cell composed of a dialysis membrane filled with milliQ water with its two electrodes (platinum and copper rods; see Figures 4 and 7 for the core of the separating apparatus;

images of the entire equipment are reported in the ESI, Figures S3-S4). The colloid (volume = 6 mL) was then charged into the funnel, the electrolytic cell immersed therein, and connected to the DC power supply. To our delight, after turning on the power (constant current: 70 mA), electrolysis occurred within the cell and NPs coagulated outside the membrane at the bottom of the funnel with minimal membrane EPD.[29]

Optimal conditions for NP coagulation were found from a set of experiments with water electrolysis at either constant current or potential. The parameters considered were: i) the mass recovery of coagulated **NP1s-(a)** and those left in the clarified liquor; ii) the pH of the clarified solution; iii) the d_h and Z_p of separated and re-dispersed NPs, and iv) the NPs sedimentation rate (section 4 in the ESI). Efficient separations were obtained by minimizing membrane EPD, which remained negligible below 100 mA constant current or 25 V constant potential, while becoming significant at values above 150 mA or 30 V, respectively. The best compromise between coagulation time and mass recovery was achieved with 90 mA or 24 V. Under these conditions, recovery of coagulated **NP1s-(a)** was ≥ 95% (w/w) within 60 minutes (Figure 4 , top).

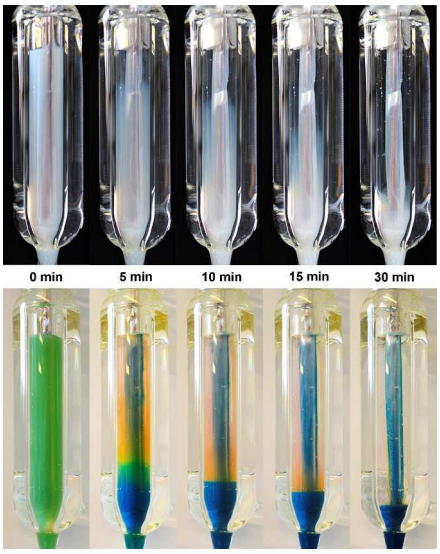

Figure 4. Evolution (30 min) of **NP1-(a)** membrane mediated-electrocoagulation (constant current: 90 mA) under batch conditions without (top) and with (bottom) universal pH indicator (green: neutral; blue: basic; yellow: weakly acid). A time-lapse video showing a direct comparison of the two experiments is available in the ESI.

The color changes observed in a membrane-mediated EC control experiment in the presence of universal pH indicator (Figure 4, bottom) confirmed the desired membrane-mediated ion flow and, at the same time, indicated Br^- to OH^- ion exchange on the external shell of **NP1s**, confirmed by the moderate acidity (pH *ca.* 3.5) of the clarified solution and Br^- precipitation with $AgNO_3$. Coagulated and separated **NP1s** could be redispersed in milliQ water with only a small Z_p decrease (3%) and moderate d_h increase (22%). As expected, a basic re-suspended NP colloid was obtained (pH *ca.* 9.0) starting from an almost neutral suspension of **NP1s-(a)** (Figure 5).

Figure 5. Left vial: coagulated/redispersed **NP1s-(a)**. Right vial: clarified liquor.

The overall series of reactions occurring during the membrane-mediated EC of **NP1s** is depicted in Scheme 2. Protons and hydroxyl ions generated within the electrolytic cell (H^+_{in} and OH^-_{in}) flow into the colloid bulk (H^+_{out} and OH^-_{out}) and equilibrate across the membrane; then, the OH^-_{out} ions exchange with Br^- on the **NP1** shell. Gratifyingly, the coagulated and redispersed basic **NP1s** were successfully electrocoagulated under the same conditions.[30]

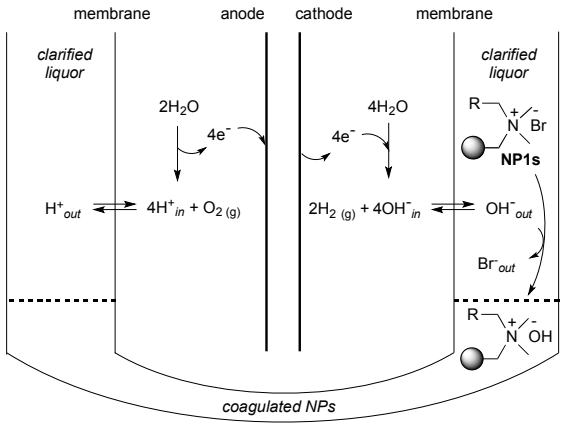

Scheme 2. Reactions occurring during the membrane-mediated electrocoagulation of **NP1s** (R = C_7H_{15}).

Organo-photocatalysis and recycle of nano-supported catalyst

The above findings paved the way for an effective approach to the recover and recycle nanocatalysts supported on CS-PMMA NPs. A specific case study was selected to investigate its feasibility in organo-photocatalysis. Photocatalytic reactions in water medium with molecular oxygen (air) as oxidant are important within the realm of green chemistry, but quite rare in the field of organic synthesis.[31] In particular, a synthetic methodology using nano-supported organo-photocatalysts is unprecedented to the best of our knowledge. Therefore, the ability of **NP2s** to promote oxygen photoexcitation in aqueous media was tested in the aerobic oxidation of the model sulfide **6** to the corresponding sulfoxide **7** (Scheme 3).

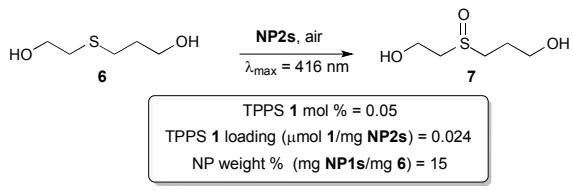

Scheme 3. Nanocatalytic -sulfoxidation of sulfide **6** in water medium.

To this aim, **NP2** colloids were prepared with various loadings of TPPS **1** by simply adding solutions at different concentrations of **1** to the **NP1-(b)** colloid under vigorous magnetic stirring. As we previously observed for similar TPPS-loaded NPs, the Br^- to TPPS ion exchange on the NPs surface was confirmed by argentometric titration.[19] Moreover, the absence of unbound TPPS **1** was confirmed at the end of the immobilization step by UV/Vis analysis (Figure S8). Furthermore, control experiments excluded any catalytic activity of the unloaded **NP1** and any reactivity in the dark and/or without dissolved oxygen using **NP2s** (section 6 in the ESI for details). Reactions bubbled with air or pure oxygen showed comparable kinetics while no bubbling resulted in slower oxidations, accounting for the lower reaction rates in the continuous flow procedure (see below). With a suitable light source (Giesemann PowerChrome Pure Actinic; λ_{max} = 416 nm), the oxidation/purification process was optimized considering three main reaction parameters: TPPS **1** mol % (μmol of **1** per μmol of **6**), TPPS **1** loading (μmol of **1** per mg of **NP1**), and NP weight % (mg of **NP1** per mg of **6**). While the first two parameters are strictly related to intrinsic factors of the reaction (conversion and selectivity), the last one is associated with extrinsic factors (sustainability, safety, time, and cost of NP processing). Both intrinsic and extrinsic factors contribute to the chemical efficiency (CE)[32] of the photo-oxidation process. This key aspect was quantified on the basis of Equation (1), where $t_{50\%}$ corresponds to the half-conversion time of **6**.

$$\mathrm{CE} = \frac{\text{conversion} \times \text{selectivity}}{\mathbf{1}\ \text{mol\%} \times \mathbf{1}\ \text{loading\ \%} \times \text{NP weight\ \%} \times t_{50\%}} \qquad (1)$$

The results of the optimization study are summarized in section 7 of the ESI. The best reaction conditions, which are highlighted in the box of Scheme 3, gave the target sulfoxide **7** in quantitative yield in 60 min as determined by NMR analysis. It is important to emphasize that the photo-sulfoxidation of **6** proceeded with only 0.05 mol% of supported TPPS **1** affording **7** without any trace of the corresponding sulfone.[33]

After having established the optimal reaction conditions, the performance of the previously disclosed membrane-mediated EC method was next evaluated in the processing of crude sulfoxidation mixtures for the efficient isolation of product **7** (Table 2). A preliminary and fundamental EC experiment with neat **NP2s** (24 V, 1 h; entry 1) showed recovered NPs (97 w/w%) with unmodified d_h, □□, UV/Vis absorption spectrum (Figure 6) and no release of TPPS **1** in the clarified liquor. Notably, in sharp contrast to the Br^-/OH^- ion exchange previously observed with unloaded **NP1s**, this result evidenced the crucial importance of the tetrasulfonate groups in TPPS **1** for the stability of the nano-catalyst **NP2**.

Application of the membrane-mediated EC method to the processing of the optimized photo-sulfoxidation of **6** resulted in the effective clarification of the colloid but in a troublesome isolation of product **7**. Indeed, 16% of **7** diffused into the membrane; this expected phenomenon, together with the unavoidable loss of **7** (18%) in the coagulated NP phase contributed to an unsatisfactory isolated yield of **7** (66%, entry 2).

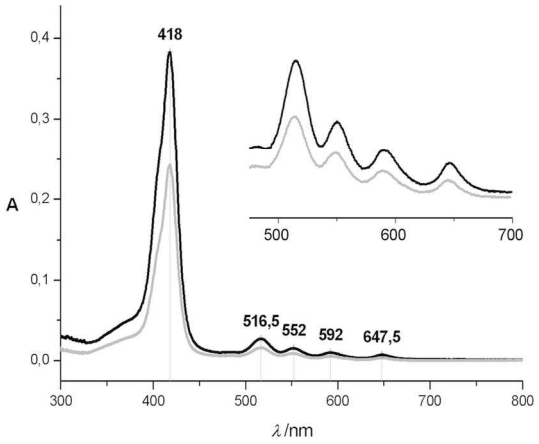

Figure 6. UV/Vis absorption spectra of **NP2s** before (black trace) and after (grey trace) membrane-mediated electrocoagulation.

A more efficient EC procedure for the recovery of **7** was successfully attempted using a continuous-flow approach. By keeping the DC power supply on, the crude batch reaction and pure water were simultaneously and independently fed at different flow rates at the bottom of the separating apparatus (Figure 7). In these experiments, **NP2s** accumulated below the membrane without any filtering medium, allowing the clarified liquor to be continually collected from the overflow. The continuous washing of coagulated **NP2s** with fresh flowing water extracted **7** from the NP deposit while limiting its diffusion into the membrane.

Table 2. Performance of the batch and flow EC-based processing of neat **NP2s** and crude sulfoxidation mixtures.

Entry	EC Procedure[a]	Isolated **7** [yield %]	**7** in NPs [yield %]	**7** in membr. [yield %]	Rec. **NP2** [w/w %][b]
1	batch[c]	/	/	/	97
2	batch[d]	66	18	16	97
3	flow[c,e]	/	/	/	96
4	flow[d]	91	6	3	92
5	flow[f,g]	92	5	3	87
6	flow[f,h]	89	8	3	75[i]

[a]Membrane-mediated electrocoagulation (EC) conditions. [b]**NP2** recovery after EC. [c]EC performed with neat **NP2s**. [d]Batch reaction processed. [e]No washing water. [f]Flow reaction processed. [g]1st cycle. [h]2nd cycle. [i]Based on **NP2s** recovered after the 1st cycle.

Again, a preliminary blank experiment with neat **NP2s** was propaedeutic for the optimization of this approach. Hence, the **NP2** colloid was fed (180 μL/min) into the separatory funnel

with the power of the electrolytic cell turned on at the constant voltage of 24 V. Gratifyingly, under these optimal conditions, 96% (w/w) of **NP2s** were recovered with unmodified d_h and □□ (entry 3). In a subsequent experiment, neat **NP2s** were replaced in the inlet stream (30 μL/min) with the colloidal sulfoxidation mixture and fresh washing water was simultaneously fed (150 μL/min) into the separatory apparatus by a dual syringe pump. The best water/crude ratio (5:1) was set on the basis of the isolated **7** (91%), whose diffusion into the membrane (3%) and dispersion in the coagulated NP phase (6%) were considerably reduced (entry 4). A time-lapse video showing the optimized continuous-flow reaction processing is available in the ESI.

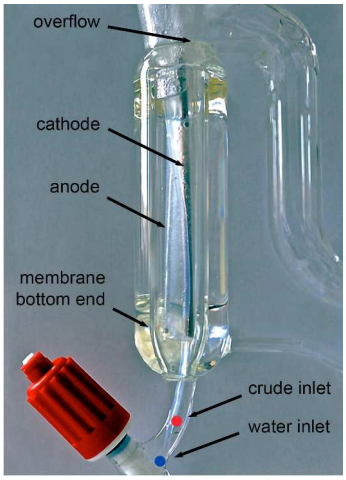

Figure 7. Details of the experimental set-up for the continuous-flow reaction processing.

This observed improvement prompted us to design a suitable meso-flow photo-reactor for the continuous production/purification of **7**. Accordingly, a fluorinated ethylene polymer (FEP) tubing (1.0 mm ID) was wrapped around a quartz cylinder holding the lamp (Figures S15 and S16). On going from batch to continuous-flow reaction conditions, full conversion of sulfide **6** occurred with a residence time of 6 hours (selection of the operative parameters for the continuous-flow sulfoxidation/EC process is described in section 13 of the ESI). As already discussed, the observed slower kinetics of the model sulfoxidation in flow regime was determined by the low concentration of oxygen in the flowing reaction stream. Unfortunately, purging the reaction mixture with oxygen before irradiation and/or continuously adding oxygen into the inlet stream through a gastight syringe and T-mixer did not produce any significant improvement.[34] Nevertheless, the effectiveness of the continuous-flow production/purification of **7** was confirmed in an experiment with a photo-reactor of proper volume (10.8 mL, 13.8 m tube length), which allowed for an outlet stream of the colloidal mixture into the separating apparatus with the desired flow-rate (30 μL/min). As expected, the simultaneous feeding of water (150 μL/min) permitted the continuous separation of **7**, which was isolated in 92% yield (entry 5). Remarkably, the coagulated, separated (mass recovery: 87 w/w%), and redispersed **NP2s** displayed the same catalytic activity of freshly prepared **NP2** colloids. This was demonstrated by a recycling experiment performed under the optimized flow conditions, which produced the sulfoxide **7** in 89% isolated yield (entry 6).

Conclusions

In summary, we have presented a novel application of core-shell poly-methylmethacrylate nanoparticle (CS-PMMA NP) of type **NP1** as inert, polymeric nano-support for the immobilization of charged (organo)catalysts and disclosed a mild, inexpensive, and sustainable procedure for the recovery of the resulting nanocatalyst from aqueous colloids. The NP separation technique, herein named membrane-mediated electrocoagulation (EC), was based on a new variant of electrocoagulation, effected through water electrolysis and mediated by an ion-permeable membrane. The efficacy of the disclosed NP processing method was tested in a continuous-flow reaction/separation/recycle sequence with the nano-supported organo-photocatalyst **NP2** displaying the tetraphenylporphyrin tetrasulfonate (TPPS) **1** as active species. Moreover, the capability of **NP2** to promote oxygen photoexcitation in water media was first demonstrated using the sulfoxidation of a model sulfide as the benchmark. Then, execution of the optimized synthetic/purification sequence allowed for the continuous production of the target sulfoxide in a pure form with no need of extracting solvents, and also the almost complete recovery of nanocatalyst **NP2** without significant loss of activity.

While further studies are currently in progress to improve the engineering aspects of the whole procedure with the aim to reduce the residence time of the continuous-flow process and enhance the recyclability of the catalyst, we believe this proof of concept may represent an initial, useful contribution to the current search for more efficient, economic, and environmentally benign production strategies based on nanocatalysis.

Experimental section

Solvents were dried over standard drying agent and freshly distilled prior to use. Deionized water was obtained with milli-Q Millipore Water Purification System and is referred as milliQ water throughout the paper. Flash chromatography was performed on Teledyne Isco CombiFlash® R_f 200 using RediSep® Normal-phase Silica Flash Columns (230-400 mesh). Reactions were monitored by TLC on silica gel 60 F_{254} with detection by charring with $KMnO_4$. Hydrodynamic diameters were determined by dynamic light scattering (DLS) at 25 °C using a sizer 3000 HS system (Malvern, UK) equipped with a 10 mV He–Ne laser. Data were analyzed based on the viscosity and refractive index of pure water at 25°C. The instrument was calibrated with standard polystyrene latex particles of 200 nm in diameter. Zeta-potentials (Z_p) were measured at 25°C by means of the same Zetasizer 3000 HS system. The instrument

calibration was checked using standard polystyrene latexes, supplied by Malvern Instruments with known Z_p. Quaternary ammonium salt loading per gram of NPs was determined by potentiometric titration of the bromide ions obtained after complete ion exchange. The ionic exchange was accomplished by dispersing the NPs sample in 1M KNO_3 at room temperature. In these conditions, a quantitative ionic exchange was achieved. The mixture was then adjusted to pH 2 with conc. H_2SO_4 and bromide ions were titrated with a 0.02 M solution of $AgNO_3$. SEM analyses were performed with a Zeiss Gemini 1530 scanning electron microscope. AFM images were performed in air and recorded using a Multimode IIIA (Bruker) scanning probe. Imaging was done in tapping mode using a silicon RTESPA probe (Bruker, frequency f0 = 270 KHz and nominal tip radius ≤ 15 nm). UV spectra were registered with a Lambda 20 Perkin Elmer spectrophotometer. NMR spectra were recorded in $CDCl_3$ or D_2O solutions at 25°C on a Varian Mercury spectrometer operating at 400 MHz (^1H) and 100.5 MHz (^{13}C). Water signal in ^1H NMR spectra of wet samples was suppressed using presat pulse sequence (optimized parameters: d_1=0, satpwr=6, satdly=4, sspul="y"). IR spectra were registered with a Perkin Elmer Spectrum BX FT-IR System. For accurate mass measurements, the compounds were analyzed in positive ion mode by Agilent 6520 HPLC-Chip Q/TOF-MS (nanospray) using a quadrupole, a hexapole, and a time-of-flight unit to produce spectra. The capillary source voltage was set at 1700 V; the gas temperature and drying gas were kept at 350°C and 5 L/min, respectively. MS analyzer was externally calibrated with ESI-L low concentration tuning mix from m/z 118 to 2700 to yield accuracy below 5 ppm. Accurate mass data were collected by directly infusing samples in 40/60 H_2O/ACN 0.1% TFA into the system at a flow-rate of 0.4 □L/min. FEP tubing, 1/16" × 1.0 mm ID and PTFE tubing, 1/16" × 1.0 mm ID were purchased from VICI Jour. UV CLEO 15 W lamp was produced by Philips. 11 W 6400 K CFL (Compact Fluorescent Lamp) was produced by Lexman. PowerChrome Pure Actinic 24 W T5 lamp was produced by Giesemann. The emission spectra of the lamps were registered using an Edinburgh FLS920 spectrometer equipped with a Peltier-cooled Hamamatsu R 928 photomultiplier tube (sensitive in the 185–850 nm range). The excitation source was off during the acquisition. Photoinduced reactions were carried out open to air in a glass vial (diameter: 1 cm [4 mL] or 2.5 cm [20 mL]; wall thickness: 0.65 mm) directly lied on lamps. Faber-Castell TK9071 2B leads (Φ = 2 mm, length = 13 cm) were used as graphite rods. (Copper rods (Φ = 2 mm, length = 25 cm, copper welding rods) was produced by KEMPER GROUP. Platinum rod (Φ = 1 mm, length = 25 cm) were purchased from Metalli Preziosi SpA. DC-current was supplied by a QJE QJ3005C 0-30VDC/0-5A, stabilized DC power supply. Voltage was measured with a EXITV EX-845 cod. 85001030 auto-range digital multimeter. Current intensity was measured with an Electraline 4-digit 59002 digital multimeter. The dialysis membranes (Medicell International Ltd dialysis Visking tubing; Φ□□= 6.3 mm or Φ□□= 28.6 mm; MWCO = 12-14 KDa) were washed in running water for 3 - 4 hours before using. A Mettler Toledo SevenMulti pH-meter was used for pH measurements. In continuous-flow experiments reagents and washing water were fed using an Harvard Apparatus 22 syringe dual. All chemicals were purchased from Sigma-Aldrich.

Caution: the membrane-mediated electrocoagulation method results in the generation of a small amount of hydrogen gas, which is a potential fire hazard.

2-(dimethyloctyl) ammonium ethylmethacrylate bromide (4).

2- (dimethylamino)ethylmethacrylate (DMAEMA) **2** (26.1 g, 0.17 mol) was mixed with neat 1-bromooctane **3** (16.0 g, 0.083 mol) and 2,6-di-tert-butyl-4-methylphenol (BHT, 8 mg, 0.036 mmol). The mixture was stirred at 50°C for 24 h; then, the resulting solid product was washed with dry diethyl ether, crystallized in acetone, and dried under vacuum to obtain **4**[20a] (17.7 g, 61%) as a pure solid. ^1H NMR ($CDCl_3$): δ = 6.12 (t, *J* = 1.1 Hz, 1 H), 5.63 - 5.70 (m, 1 H), 4.58 - 4.70 (m, 2 H), 4.11 - 4.21 (m, 2 H), 3.57 - 3.67 (m, 2 H), 3.51 (s, 6 H), 1.93 (dd, *J* = 1.5, 0.9 Hz, 3 H), 1.66 - 1.81 (m, 2 H), 1.13 - 1.43 (m, 10 H), 0.80 - 0.91 (m, 3 H). ^{13}C NMR ($CDCl_3$): δ = 166.5, 135.4, 127.6, 65.7, 62.4, 58.3, 52.1, 31.8, 29.4, 29.2, 26.5, 23.2, 22.8, 18.5, 14.2.

Synthesis of NP1s-(a) and NP1s-(b).

A 4-necked 250 mL round bottomed flask equipped with a mechanical stirrer, a thermometer, a nitrogen inlet and a condenser, was charged with 2-(dimethyloctyl) ammonium ethylmethacrylate bromide **4** and distilled water (100 mL). The mixture was then heated. Upon reaching 80°C, nitrogen was bubbled in the solution bulk for 10 min. Methyl methacrylate (MMA) **5** was then added dropwise into the stirred reaction mixture under nitrogen atmosphere. After 15 min, 2,2′-azobis (isobutyramidine) dihydrochloride (AIBA) was added thereto. The obtained white suspension was stirred at 80°C for additional 4 h. After cooling at room temperature, the milky suspension was dialyzed for 15 days changing the outer water 2 times a day (dialysis Visking tubing;□Φ□□= 28.6 mm; MWCO = 12-14 KDa). **NP1s-(a)**: MMA **5** (5.0 mL, 53 mmol); **4** (1.02 g, 2.90 mmol); AIBA (13 mg, 0.048 mmol). **NP1s-(b)**: MMA **5** (2.0 mL, 19 mmol); **4** (1.02 g, 2.90 mmol); AIBA (15 mg, 0.055 mmol). See Table 1 for hydrodynamic diameters, Zeta potentials, and concentrations.

Experimental set-up for the membrane-mediated electrocoagulation under batch conditions.

Electrolytic cell (Figure S3a): a copper rod (Φ□= 2 mm) and a platinum rod (Φ□= 1 mm), separated by a dielectric spacer (polypropylene [PP], thickness = 0.8 mm) and aligned at the distance of 3 mm, were inserted into a bottom-end sealed dialysis membrane (Visking tubing, MWCO = 12-14 KDa, Φ□= 6.3 mm). The membrane was filled with 2.0 □L of milliQ water. When connected to the DC power supply, the copper rod worked as the cathode and the platinum rod as the anode. A custom made cap (Figures S3b), equipped with a 29/32 cone on the bottom, two eccentric inlets on the top, one coaxial, and two

perpendicular pipes on the body, was used as holder for the electrolytic cell. A custom made dropping funnel (Figure S3c), equipped with a thermostatic jacket, a Rotaflow Stopcock on the bottom, an overflow pipe, and a 29/32 socket on the top was used as the *settling device*. The final *separating apparatus* (Figure S3d) was assembled when the electrodes holder was fixed on the top of the settling device.

Membrane-mediated electrocoagulation of NP1s-(a) under batch conditions (constant current or voltage).

A 5.05 mg/mL suspension of **NP1s-(a)** was obtained diluting 3.0 mL of **NP1s-(a)** starting colloid in 15.0 mL of milliQ water. 6.0 mL of the diluted colloid were placed into the *settling device*. The *electrolytic cell* was immersed therein and DC was supplied. All experiments were run at constant DC or constant voltage (Table S3). During each run, the following parameters were monitored: the current flowing in the electrolytic cell, the voltage across the electrodes, the up-front height of the settling colloid and, starting from when it became recognizable, the thickness of the settling area (Figure S4). After 60 min, and with the power still on, the clarified liquor was withdrawn from the top of the separating apparatus at the flow-rate of 1.4 mL/min. This was an optimized procedure to limit NP remixing during the separation of the two phases. All recovered clarified liquors were diluted at the final volume of 5.0 mL. The settled colloids of coagulated **NP1s-(a)** were recovered and diluted at the final volume of 9.0 mL. The pH of both recovered **NP1s-(a)** and clarified liquors were finally measured. After each experiment, two portions of an exactly known volume of both recovered **NP1s-(a)** and clarified liquors were freeze-dried in pre-tared vials for the gravimetric analysis (Table S3).

Synthesis of NP2s.

A 0.1 mg/mL solution of TPPS **1** was initially prepared by dissolving 0.86 mg of TPPS **1** in 8.6 mL of milliQ water. Under vigorous magnetic stirring, 4.50 mL of the TPPS **1** solution (449 μg, 0.44 μmol) were added drop-wise to the **NP1-(b)** starting colloid [1.23 □L of a 14.6 mg/mL colloid corresponding to 18.0 mg of **NP1s-(b)**]. 0.47 mL of additional milliQ water were added to the purple colored colloid to obtain the final nanocatalyst **NP2** [concentration = 2.9 mg/mL; TPPS **1** loading = 0.024 (μmol **1**/mg **NP1s-(b)**)]. See Table 1 for hydrodynamic diameter and Zeta potential.

Membrane-mediated electrocoagulation of NP2s under batch conditions.

6.0 mL of freshly prepared **NP2s** (see the above section) were placed into the *settling device*. The *electrolytic cell* was immersed therein and a constant voltage of 24.0 V was supplied. After 1 h and with the power still on, the clarified liquor was withdrawn from the top of the separating apparatus at the flow-rate of 1.4 mL/min. The recovered clarified liquor was diluted at the final volume of 5.0 mL. The settled colloid of coagulated **NP2s** was recovered and diluted at the final volume of 9.0 mL. The pH of both coagulated **NP2s** and clarified liquor were finally measured. Two portions of an exactly known volume of both recovered **NP2s** and clarified liquor were freeze-dried in pre-tared vials for the gravimetric analysis (Table S7).

Optimized sulfoxidation/purification procedure under batch conditions (Table 2, entry 2).

6.2 mL of a **NP2** colloid were freshly prepared as previously described. In a 20 mL vial, the obtained colloid was added to the sulfide **6** (122 mg, 0.90 mmol). The resulting reaction mixture was irradiated (Giesemann PowerChrome Pure Actinic 24 W T5 lamp) at room temperature while compressed air was bubbled therein (air flow-rate: 240 mL/min). After 120 min, ^{1}H NMR analysis of the crude reaction mixture indicated the following products distribution: sulfide **6**, 2.1 mol %; sulfoxide **7**, 97.7 mol %; sulfone **8**, 0.16 mol %. The crude mixture was then charged into the *settling device* and the *electrolytic cell* was immersed therein. The power was turned on at the constant DC of 100.0 mA. After 1 h and with the power still on, the clarified liquor was withdrawn from the top of the separating apparatus at the flow-rate of 1.4 mL/min. The recovered clarified liquor (5.4 mL), the water in the membrane, and the coagulated **NP2s** were freeze-dried to evaluate the distribution of product **7** in these phases (Table 2, entry 2). The amount of **7** in coagulated **NP2s** was determined by difference and confirmed by ^{1}H NMR analysis of this phase using methanol as the internal standard. Recovered 3-((2-hydroxyethyl)sulfinyl)propan-1-ol **7** in the clarified liquor: 90 mg, 66%. ^{1}H NMR (D_2O): δ = 3.83 - 3.95 (m, 2 H), 3.62 (t, J = 6.5 Hz, 2 H), 2.97 - 3.07 (m, 1 H), 2.78 - 2.96 (m, 3 H), 1.83 - 1.93 (m, 2 H). ^{13}C NMR (D_2O): δ = 60.2, 54.9, 53.8, 48.0, 25.0. HRMS (ESI) *m/z* calcd for $C_5H_{13}O_3S$ $[M+H]^+$ 153.0585, found: 153.0612.

Experimental set-up for the membrane-mediated electrocoagulation of NP2s under flow conditions.

The *settling device* was charged with 6.0 □L of milliQ water and the *electrolytic cell* immersed therein. The inlet of a first PTFE tubing (OD 1/16" x 1.00 mm ID) was connected to a 10.0 mL gastight syringe filled with **NP2** colloid (Table 2, entry 3) or with the reaction mixture (batch reaction; Table 2, entry 4). Otherwise, the same tube (FEP) was part of the photo-reactor (flow reactions; Table 2, entries 5 and 6). The outlet of the first tubing was immersed in the *separating apparatus*, below the bottom of the membrane. The inlet of a second PTFE tubing (OD 1/16" x 1.00 mm ID) was connected to a 50.0 mL gastight syringe filled with milliQ water. The outlet of the same PTFE tubing was immersed in the *separating apparatus*, below the first PTFE tubing (Figure 4).

Membrane-mediated electrocoagulation of NP2s under flow conditions (Table 2, entry 3).

The *settling device* was charged with 6.0 □L of milliQ water and the *electrolytic cell* immersed therein. 7.0 mL of the **NP2** colloid were freshly prepared as previously described and charged in the 10.0 mL gastight syringe; in parallel, 35.0 mL of milliQ water were charged in the 50.0 mL gastight syringe. The

power in the electrolytic cell was turned on at constant voltage (24.0 V). Using a dual syringe pump, both the **NP2** colloid (flow-rate: 30 μL/min) and the washing water (flow-rate: 150 μL/min) were fed into the *separating apparatus* (overall flow-rate: 180 μL/min). During electrocoagulation, **NP2s** remained trapped below the bottom of the membrane, while the clarified liquor was collected through the overflow. After 233 min (3 h 53 min) 42.0 mL of clarified liquor were collected. The trapped and washed **NP2s** were diluted with milliQ water to obtain 13.0 mL of the colloid. Both the clarified liquor and the recovered colloid were freeze-dried for the gravimetric analysis.

Optimized sulfoxidation/purification procedure under flow conditions (Table 2, entry 5).

The settling *device* was charged with 6.0 □L of milliQ water and the *electrolytic cell* was immersed therein. 13.8 m of FEP tubing (OD 1/16" x 1.0 mm ID; 10.8 mL) was wrapped in a single layer around a quartz tube holding the Giesemann PowerChrome Pure Actinic 24 W T5 lamp to build-up the photo-reactor. Additional 1.50 m of FEP tubing were used for the connection with a 10.0 mL gastight syringe (inlet) and for the collection in the separating apparatus (outlet) below the bottom of the membrane. The inlet of a second PTFE tubing (OD 1/16" x 1.00 mm ID) was connected to a 50.0 mL gastight syringe filled with milliQ water, while the outlet was immersed in the *separating apparatus* below the outlet of FEP tubing coming from the photo-reactor. Both syringes were placed in the dual syringe pump apparatus. The *flow reactor/separating apparatus* is depicted in Figure S16.

6.0 mL of the **NP2** colloid were freshly prepared as previously described. In a 20 mL vial, the obtained colloid was added to sulfide **6** (121 mg, 0.89 mmol). The resulting reaction mixture was charged into the 10.0 mL gastight syringe and fed in the FEP photo-reactor at the flow-rate of 30 μL/min (residence time: 360 min). When the crude mixture started to flow inside the separating apparatus, the power in the electrolytic cell was turned on (100 mA constant DC) and the washing water was fed in the separating apparatus at the flow-rate of 150 μL/min. Once the addition of the crude reaction mixture was completed, pure water was pumped inside the separating apparatus at 180 μL/min for 15 min.

At the end of the experiment, the purified solution of **7**, which was collected from the overflow, the water contained in the membrane, and **NP2s** trapped below the membrane were independently freeze-dried. The amount of **7** in coagulated **NP2s** was determined by difference and confirmed by ^{1}H NMR analysis of this phase using methanol as the internal standard. Recovered 3-((2-hydroxyethyl)sulfinyl)propan-1-ol **7** from the overflow: 124 mg, 92%.

Continuous-flow recycle experiment (Table 2, entry 6).

NP2s trapped below the membrane after the first continuous flow reaction/electrocoagulation cycle were transferred in a 20 mL vial, diluted to 6.0 mL with milliQ water, and added to sulfide **6** (121 mg, 0.89 mmol). The recycle experiment was performed as described affording **7** from the overflow: 12 mg, 89%.

Acknowledgements

We thank Dr. Luisa Pasti (UNIFE), Dr. Alberto Zanelli (ISOF), Dr. Vincenzo Palermo (ISOF), Dr. Derek Jones (ISOF), Dr. Alfredo Ventola (AcZon srl) for useful discussions, Mr. Franco Corticelli (IMM-CNR) for SEM measurements, and Dr. Andrea Liscio (ISOF) for AFM measurements. Mr. Silvano Favaretto (ISOF), Mr. Giovanni Bragaglia (ISOF), Mr. Maurizio Ghirardelli (ISOF), Mr. Paolo Formaglio (UNIFE), and Dr. Tatiana Bernardi (UNIFE) are gratefully acknowledged for technical assistance.

Notes and references

[a]Istituto per la Sintesi Organica e la Fotoreattività, Consiglio Nazionale delle Ricerche, Via P. Gobetti, 101 – 40129 – Bologna (Italy). E-mail: paolo.dambruoso@isof.cnr.it.

[b]Dipartimento di Scienze Chimiche e Farmaceutiche, Università di Ferrara, Via Fossato di Mortara, 17 – 44121 – Ferrara (Italy). E-mail: alessandro.massi@unife.it.

†Dedicated to the memory of Arturo Battaglia, our dear friend and mentor, and his wife Maria Grazia Allegri.

‡Electronic Supplementary Information (ESI) available: Experimental procedures, SEM, AFM, spectroscopic data. See DOI: 10.1039/b000000x/

1 (*a*) Q. M. Kainz and O. Reiser, *Acc. Chem. Res.*, 2014, **2**, 667; (*b*) I. R. Baxendale, L. Brocken and C. J. Mallia, *Green Process. Synth.,* 2013, **2**, 211; (*c*) M. O'Brien, R. Denton and S. V. Ley, *Synthesis*, 2011, **2011**, 1157; (*d*) A. Kirschning, W. Solodenko and K. Mennecke, *Chem. Eur. J.*, 2006, **12**, 5972.

2 (*a*) C. Jimeno, S. Sayalero and M. A. Pericas, in *Heterogenized Homogeneous Catalysts for Fine Chemicals Production: Materials and Processes*, Ed. P. Barbaro and F. Liguori, Springer Science & Business Media B. V., 2010, ch.4, pp. 123-170; (*b*) F. Cozzi, *Adv. Synth. Catal.*, 2006, **348**, 1367.

3 For selected recent reports, see: (*a*) M. Heidlindemann, G. Rulli, A. Berkessel, W. Hummel and H. Groger, *ACS Catal.*, 2014, **4**, 1099; (*b*) C. J. Whiteoak, A. H. Henseler, C. Ayats, A. W. Kleij and M. A. Pericas, *Green Chem.*, 2014, **16,** 1552; (*c*) P. O. Miranda, C. Lizandara-Pueyo and M. A. Pericas, *J. Cat.*, 2013, **305**, 169; (*d*) G. Rulli, K. A. Fredriksen, N. Duangdee, T. Bonge-Hansen, A. Berkessel and H. Groger, *Synthesis*, 2013, **45**, 2512; (*e*) P. Kasaplar, P. Riente, C. Hartmann and M. A. Pericas, *Adv. Synth. Catal.*, 2012, **354**, 2905; (*f*) A. Puglisi, M. Benaglia, R. Annunziata and J. S. Siegel, *ChemCatChem.*, 2012, **4**, 972; (*g*) S. Guizzetti, M. Benaglia and J. S. Siegel, *Chem. Comm.*, 2012, **48**, 3188; (*h*) E. Alza, S. Sayalero, P. Kasaplar, D. Almasi, and M. A. Pericas, *Chem. Eur. J.*, 2011, **17**, 11585.

4 (*a*) L. Osorio-Planes, C. Rodriguez-Escrich and M. A. Pericas, *Chem. Eur. J.*, 2014, **20**, 2367; (*b*) S. Martín, R. Porcar, E. Peris, M. I. Burguete, E. García-Verdugo and S. V. Luis, *Green Chem*., 2014, **16**, 1639; (*c*) V. Chiroli, M. Benaglia, A. Puglisi, R. Porta, R. P. Jumde

and A. Mandoli, *Green Chem.*, 2014, **16**, 2798; (*d*) T. Tsubogo, T. Ishiwata and S. Kobayashi, *Angew. Chem., Int. Ed.*, 2013, **52**, 6590; (*e*) E. Sugiono and M. Rueping, *Beilstein J. Org. Chem.,* 2013, **9**, 2457; (*f*) Y. Arakawa and H. Wennemers, *ChemSusChem*, 2013, **6**, 242; (*g*) G. Kardos and T. Soós, *Eur. J. Org. Chem*., 2013, 4490; (*h*) A. Puglisi, M. Benaglia and V. Chiroli, *Green Chem.*, 2013, **15**, 1790; (*i*) R. Martin-Rapun, S. Sayalero and M. A. Pericàs, *Green Chem.*, 2013, **15**, 3295; (*j*) M. Baghbanzadeh, T. N. Glasnov and C. O. Kappe, *J. Flow Chem.*, 2013, **3**, 109; (*k*) P. Kasaplar, C. Rodríguez-Escrich and M. A. Pericàs, *Org. Lett.*, 2013, **15**, 3498; (*l*) V. Chiroli, M. Benaglia, F. Cozzi, A. Puglisi, R. Annunziata and G. Celentano, *Org. Lett.*, 2013, **15**, 3590; (*m*) C. Ayats, A. H. Henseler and M. A. Pericàs, *ChemSusChem.*, 2012, **5**, 320; (*n*) S. B. Otvos, I. M. Mandity and F. Fulop, *ChemSusChem.*, 2012, **5**, 266; (*o*) L. Osorio-Planes, C. Rodríguez-Escrich and M. A. Pericàs, *Org. Lett.*, 2012, **14**, 1816; (*p*) A. L. W. Demuynck, L. Peng, F. de Clippel and J. Vanderleyden, *Adv. Synth. Catal.*, 2011, **353**, 725; (*q*) X. C. Cambeiro, R. Martin-Rapun, P. O. Miranda, S. Sayalero, E. Alza, P. Llanes and M. A. Pericàs, *Beilstein J. Org. Chem.,* 2011, **7**, 1486; (*r*) E. Alza, S. Sayalero, X. C. Cambeiro, R. Martin-Rapun, P. O. Miranda and M. A. Pericas, *Synlett*, 2011, **2011**, 464; (*s*) E. Alza, C. Rodríguez-Escrich, S. Sayalero, A. Bastero and M. A. Pericàs, *Chem. Eur. J.*, 2009, **15**, 10167; (*t*) F. Bonfils, I. Cazaux, P. Hodge and C. Caze, *Org. Biomol. Chem*., 2006, **4**, 493; (*u*) S. France, D. Bernstein, A. Weatherwax and T. Lectka, *Org. Lett.*, 2005, **7**, 3009; (*v*) D. Bernstein, S. France, J. Wolfer and T. Lectka, *Tetrahedron: Asymmetry*, 2005, **16**, 3481; (*w*) A. M. Hafez, A. E. Taggi, T. Dudding and T. Lectka, *J. Am. Chem. Soc.*, 2001, **123**, 18853.

5 (*a*) L. Zhang, L. Cui, S. Luo and J.-P. Cheng, in *Green Techniques for Organic Synthesis and Medicinal Chemistry,* Ed. W. Zhang and B. W. Cue Jr., John Wiley & Sons, Ltd., 2012, ch. 5, pp. 99-135; (*b*) R. Porta, M. Benaglia, V. Chiroli, F. Coccia and A. Puglisi, *Israel J. Chem.*, 2014, **54**, 381; (*c*) S. Mondini, A. Puglisi, M. Benaglia, D. Ramella, C. Drago, A. M. Ferretti and A. Ponti, *J. Nanopart. Res.*, 2013, **15**, 2025; (*d*) A. Puglisi, M. Benaglia, R. Annunziata, V. Chiroli, R. Porta and A. Gervasini, *J. Org. Chem.*, 2013, **78**, 11326; (*e*) B. H. Lipshutz and S. Ghorai, *Org. Lett.*, 2012, **14**, 422; (*f*) P. Riente, J.Yadav and M. A. Pericas, *Org. Lett.*, 2012, **14**, 3668; (*g*) P. Riente, C. Mendoza and M. A. Pericas, *J. Mater. Chem.*, 2011, **21**, 7350; (*h*) A. Puglisi, R. Annunziata, M. Benaglia, F. Cozzi, A. Gervasini, V. Bertacche and M. C. Sala, *Adv. Synth. Catal.*, 2009, **351,** 219; (*i*) O. Gleeson, R. Tekoriute, Y. K. Gun'ko and S. J. Connon, *Chem. Eur. J.*, 2009, **15**, 5669; (*j*) B. Zhao, X. Jiang , D. Li, X. Jiang, T. G. O'Lenick, B. Li and C. Y. Li, *J. Polym. Sci., Part A: Polym. Chem.*, 2008, **46**, 3438.

6 D. Astruc, F. Lu and J. R. Aranzaes, *Angew. Chem., Int. Ed.*, 2005, **44**, 7852.

7 Selected references: (*a*) *Selective Nanocatalysts and Nanoscience*, ed. A. Zecchina, S. Bordiga and E. Groppo, VCH, Weinheim, 2011; (*b*) *Nanoparticles and Catalysis*, ed. D. Astruc, VCH, Weinheim, 2008; (*c*) L. Wu, Y. Zhang and Y. G. Ji, *Curr. Org. Chem.*, 2013, **17**, 1288.

8 For selected reviews, see: S. Shylesh, V. Schünemann and W. R. Thiel, *Angew. Chem. Int. Ed.*, 2010, **49**, 3428; (b) A. Schätz, O. Reiser and W. J. Stark, *Chem. Eur. J.*, 2010, **16**, 8950.

9 I. Geukens, D. E. De Vos, in *Nanomaterials in Catalysis,* ed. P. Serp and K. Philippot, VCH, Weinheim, 2013, ch. 8, pp. 311–330.

10 D. Obermayer, A. M. Balu, A. A. Romero, W. Goessler, R. Luque and C. O. Kappe, *Green Chem.*, 2013, **15**, 1530.

11 E. Gross, J. H.-C. Liu, F. D. Toste and G. A. Somorjai, *Nat. Chem.*, 2012, **4**, 947.

12 J. D. Bass, X. Ai, A. Bagabas, P. M. Rice, T. Topuria, J. C. Scott, F. H. Alharbi, H.-C. Kim, Q. Song and R. D. Miller, *Angew. Chem., Int. Ed.*, 2011, **50**, 6538.

13 L. Besra and M. Liu, *Prog. Mater. Sci.*, 2007, **52**, 1.

14 X. Ai, J. D. Bass, H. C. Kim, R. D. Miller, J. C. Scott and Q. Song (IBM Corporation), *US Pat.*, 2011/0315553 A1, 2011.

15 R. Moreno and B. Ferrari, *Mater. Res. Bull.*, 2000, **35**, 887.

16 (*a*) O. Bortolini, A. Cavazzini, P. P. Giovannini, R. Greco, N. Marchetti, A. Massi and L. Pasti, *Chem. Eur. J.,* 2013, **19**, 7802; (*b*) O. Bortolini, A. Cavazzini, P. Dambruoso, P. P. Giovannini, L. Caciolli, A. Massi, S. Pacifico and D. Ragno, *Green Chem.,* 2013, **15**, 2981; (*c*) O. Bortolini, L. Caciolli, A. Cavazzini, V. Costa, R. Greco, A. Massi and L. Pasti, *Green Chem.,* 2012, **14**, 992; (*d*) A. Massi, A. Cavazzini, L. Del Zoppo, O. Pandoli, V. Costa, L. Pasti and P. P. Giovannini, *Tetrahedron Lett.,* 2011, **52**, 619; (*e*) A. Massi, O. Pandoli, A. Cavazzini, L. Del Zoppo, P. P. Giovannini and C. Bendazzoli, *Italian Patent*, 0001398243, 2013.

17 C. Monasterolo, M. Ballestri, G. Sotgiu, A. Guerrini, P. Dambruoso, K. Sparnacci, M. Laus, M. De Cesare, A. Pistone, G. L. Beretta, F. Zunino, V. Benfenati and G. Varchi, *Bioorg. Med. Chem.*, 2012, **20**, 6640.

18 (*a*) R. Canaparo, G. Varchi, M. Ballestri, F. Foglietta, G. Sotgiu, A. Guerrini, A. Francovich, P. Civera, R. Frairia and L. Serpe, *Int. J. Nanomed.*, 2013, **8**, 4247; (*b*) G. Varchi, V. Benfenati, A. Pistone, M. Ballestri, G. Sotgiu, A. Guerrini, P. Dambruoso, A. Liscio and B. Ventura, *Photochem. Photobiol. Sci.*, 2013, **12**, 760.

19 S. Duchi, G. Sotgiu, E. Lucarelli, M. Ballestri, B. Dozza, S. Santi, A. Guerrini, P. Dambruoso, S. Giannini, D. Donati, C. Ferroni and G. Varchi, *J. Controlled Release*, 2013, **168**, 225.

20 (a) M. Laus, K. Sparnacci, M. Lelli, R. Vannini and L. Tondelli, *J. Polym. Sci., Part A: Polym. Chem.,* 2000, **38**, 1110; (*b*) S. M. Hamid and D. C. Sherrington, *Polymer*, 1987, **28**, 325.

21 M. Gál, J. Híveš, M. Laus, K. Sparnacci, M. Ravera, E. Gabano and D. Osella, *Eur. J. Inorg. Chem.*, 2011, **2011,** 3289.

22 J. M. Fraile, J. I. García and J. A. Mayoral, *Chem. Rev.*, 2009, **109**, 360.

23 Centrifugation for 1 h at 60000 rpm of **NP1-(b)** colloids (d_h = 74 nm) afforded an unsatisfactory level of NP precipitation (2% w/w).

24 For a review, see: M. Mollah, P. Morkovsky, J. A. G. Gomes, M. Kesmez, J. Parga and D. L. Cocke, *J. Hazard. Mater.*, 2004, **114**, 199.

25 Q. Li, Y. Bao, H. Wang, F. Du, Q. Li, B. Jin and R. Bai, *Polym. Chem.*, 2013, **4**, 2891.

26 For a previous observation of this phenomenon, see: M. Arimura, T. Makino, K. Fujiyoshi, Y. Yamashita and M. Kuwabara, *Key Eng. Mater.*, 2007, **350**, 11.

27 P. Sarkar and P. S. Nicholson, *J. Am. Ceram. Soc.*, 1996, **78**, 1987.

28 A. M. Santos, A. Elaïssari, J. M. G. Martinho and C. Pichot, *Colloid Polym. Sci.*, 2004, **282**, 661.

29 P. Sarkar, O. Prakash, G. Wang and P. S. Nicholson, *Ceram. Eng. Sci. Proc.*, 1994, **15**, 1019.

30 Aqueous colloids of TiO_2 NPs and negatively charged PMMA NPs were also successfully electrocoagulated by this strategy. Results will be reported in a forthcoming paper.

31 For selected reports, see: (*a*) X. Li, X. Y. Gu, Y. J. Li and P. X. Li, *ACS Catal.*, 2014, **4**, 1897; (*b*) M. Rueping, C. Vila and T. Bootwicha, *ACS Catal.*, 2013, **3**, 1676; (*c*) X. Gu, X. Li, Y. Chai, Q. Yang, P. Li and Y. Yao, *Green Chem.*, 2013, **15**, 357; (*d*) F. Lévesque and P. H. Seeberger, *Angew. Chem., Int. Ed.*, 2012, **51**, 1706; (*e*) F. Lévesque and P. H. Seeberger, *Org. Lett.*, 2011, **13**, 5008; (*f*) J. M. Zen, S. L. Liou, A. S. Kumar and M. S. Hsia, *Angew. Chem., Int. Ed.*, 2003, **42**, 577. For a general overview on catalytic reactions in novel reaction media, see: (*g*) *Green Chemistry and Catalysis*, ed. R. Sheldon, I. W. C. E. Arends and U. Hanefeld, VCH, Weinheim, 2007.

32 J. Andraos, *Org. Process Res. Dev.*, 2005, **9**, 149.

33 **NP2** nanocatalyst successfully oxidized a variety of alkylic, aromatic, and biologically relevant sulfides. Results will be reported in a separate paper also describing the activity of a novel organo-photocatalyst supported on CS-PMMA NPs.

34 For the fabrication of a pressurized continuous-flow photoreactor allowing an increased oxygen concentration, see Ref. 30e. Pressurization by a back-pressure regulator was incompatible with our system because of the use of syringe pumps.

Photons and electrons cooperate for effective, clean sulfoxidations in pure water using a recyclable organo-photocatalyst immobilized on a polymeric nano-support, air as the terminal oxidant, and batch or continuous-flow experimental set-ups

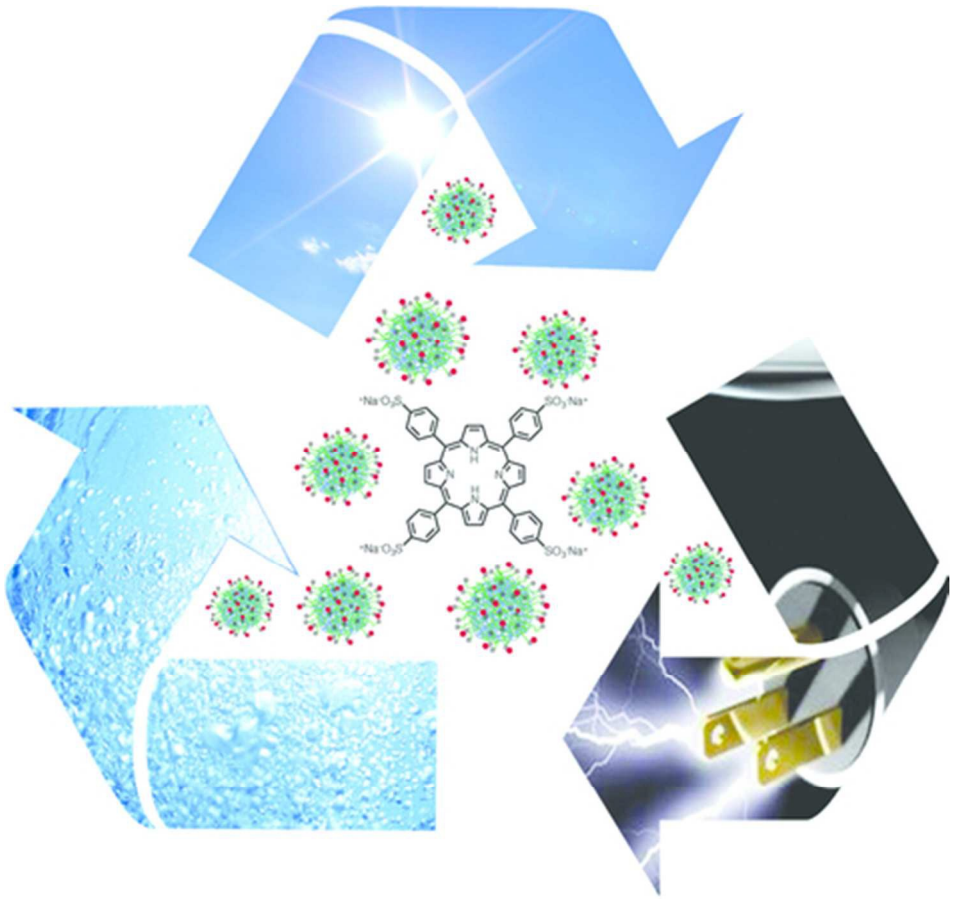

39x37mm (300 x 300 DPI)